

INVESTIGATION OF DYNAMIC GROUND EFFECT

Ray Chung Chang
Aeronautical Research Laboratory, Taichung, Taiwan

Vincent U. Muirhead
University of Kansas, Lawrence, Kansas

SUMMARY

An experimental investigation of dynamic ground effect has been conducted in the University of Kansas wind tunnel using delta wings of 60° , 70° , 75° sweep; the XB-70 wing; and the F-104A wing. Both static and dynamic tests were made. Test data have been compared to other test data, including dynamic flight test data of the XB-70 and F-104A. Limited flow visualization tests have been conducted. A significant dynamic effect was found for highly swept delta wings.

INTRODUCTION

Beginning with Fredrick W. Lanchester in 1907, the circulation theory of wing lift and the effect of wing vortices have been under study and development. The effect on the lift of a finite wing in close proximity to the ground was first studied by Weiselsberger (1922) and Tani (1937). Choliasmenos (1962) investigated the ground effect on the lift of a wing with and without boundary layer control. Abercrombie (1967) also investigated the ground effect on wings with high circulation. Both Abercrombie and Choliasmenos used rectangular wings of medium aspect ratio in their studies. Both studies concluded that the interference of the ground on wing lift was a function of the circulation of the wing when it was out of ground effect. For lift coefficients under about 2, the ground effect was favorable and above 2, unfavorable. Although Abercrombie's theory accounts for high angles of attack, it, also, is not applicable to low-aspect-ratio and highly swept wings with sharp leading edges. Fox's (1969) theory provided a good prediction of lift and drag of sharp edged planar wings near the ground in comparison with static wind tunnel data. The work of Kemp (1966), Katz (1984) and Rolls (1966) show that the current theoretical methods, static wind tunnel tests and fly-by flight tests are in reasonable agreement.

Although for high-swept low-aspect ratio wings, theoretical predictions, static wind tunnel data and fly-by flight test data are in reasonable agreement, these data do not agree with flight test landing data. Schweikhard (1967) and Baker (1970) obtained landing data with the aircraft making an approach at constant angle of attack and constant power setting. Five aircraft were tested: F5D-1, F5D-1 with a modified ogee wing, XB-70-1, XB-70-2 and F-104A. As the landing approaches were made, significant changes were found in lift, drag and pitching moment. The magnitude of these changes did not agree with theoretical and wind tunnel predictions, indicating a dynamic effect not included in the previous methods.

This paper reports on the development of a method to simulate the dynamic landing condition in the wind tunnel. It compares the dynamic wind tunnel data with

static wind tunnel data in ground effect and the flight test data of Baker (1970). Limited flow visualization tests were conducted to provide preliminary study of the phenomena involved in dynamic ground effect.

SYMBOLS

AR	wing model aspect ratio, b^2/S
b	wing model span, centimeters (inches)
\bar{b}	width of sting cross section, centimeters (inches)
$C_D = \frac{D}{qS}$	coefficient of drag in ground effect
C_{D_∞}	coefficient of drag out of ground effect
$\%C_D$	percent increase in drag coefficient, $\frac{C_D - C_{D_\infty}}{C_{D_\infty}} \times 100$
$C_L = \frac{L}{qS}$	coefficient of lift in ground effect
C_{L_0}	coefficient of lift at zero angle of attack
C_{L_∞}	coefficient of lift out of ground effect
$\%C_L$	percent increase in lift coefficient, $\frac{C_L - C_{L_\infty}}{C_{L_\infty}} \times 100$
C_M	coefficient of pitching moment about reference point in ground effect
$C_{M_\infty} = \frac{P}{qS\bar{c}}$	coefficient of pitching moment about reference point out of ground effect
C_0	wing model root chord, centimeters (inches)
\bar{c}	wing model mean geometric chord, centimeters, (inches)
D	drag, Newton's (lbs)
H	ground height, the height of the quarter chord point of the mean aerodynamic chord above the ground, centimeters (inches)
\bar{h}	height of sting cross section, centimeters (inches)

\dot{h}	sink rate, meters/sec (ft/sec)
L	lift, Newton's (lbs)
l_i	distance of the sting locations, $i = 1, 2, \dots, 5$; centimeters (inches)
P	pitching moment, meter Newton's (ft lbs)
q	dynamic pressure, Newton's/m ² (lb/ft ²)
R_N	Reynolds number based on mean aerodynamic chord
S	wing area, centimeters ² (inches ²)
y	horizontal distance from centerline of wing model, centimeters (inches)
α	angle of attack, degrees
Λ_{LE}	leading edge sweep angle, degrees

MODELS, APPARATUS AND PROCEDURE

Five model wings were tested: 60, 70 and 75 degree delta wings, Figure 1; F-104A wing, Figure 2; and XB-70 wing, Figure 3 (Chang, 1985). The models were mounted to a sting support, Figure 4, through a bracket which determined the angle of attack for the test. The sting support strut was mounted vertically in the wind tunnel in two linear bearings, Figure 5. The sting was free to move vertically between limiting stops. The sting and wing were statically counterbalanced by an external mass. By moving the mass downward, the wing moved upward in the tunnel toward a ground board. The wing was allowed to pass through a spring loaded door in the ground board at a steady sinking rate. The final travel of the sting was cushioned as the wing began to open the spring-loaded door.

Both static and dynamic tests were conducted on the five model wings. A test Reynold's number of 7×10^5 was maintained by adjusting wind tunnel speed. Static tests were conducted at angles of attack of 4, 8, 10, 15, 20, 24, 28, 30, 32, and 34 degrees at heights above the ground plane of 38.1, 15.2, 10.2, 7.6, 5.1, 3.8, 2.5 and 1.9 centimeters (15, 6, 4, 3, 2, 1.5, 1 and .75 inches). The 38.1 centimeter (15 inch) position was approximately out of ground effect.

Dynamic tests were made at angles of attack of 10, 15, 20, 24 and 28 degrees at three sink speeds: .609, 1.219, 1.828 m/sec (2, 4, and 6 ft/sec). The F-104A and XB-70 wings were also tested at 4 and 8 degrees in order to compare with available flight data.

During the dynamic tests the data from the sting (three strain gaged bridge circuits for lift, drag, and pitch, and a linear potentiometer for height) were recorded on a visicorder. An analog-digital acquisition system with a Hewlett Packard 9826 microcomputer was used to record all other data. The visicorder data were

digitized for making calculations of lift, drag, pitching moment and height. Flow visualization tests were made with neutrally buoyant helium bubbles and tufted wire grid, Figures 6 and 7.

RESULTS

The three delta wings (60, 70 and 75 degrees) had been previously tested by Wentz (1968). Figure 8 is a comparison of the lift coefficient data for the two tests of 70 degree delta wing. It will be noted that there is a marked difference in the angle of attack of stall. Figure 9 from Erickson (1982) shows that the vortex breakdown angle of attack of the Wentz tests was the largest of those reported. The current test value falls almost in the middle of the data. This illustrates the influence of small changes initial conditions: (1) the apex of the model as used in the current tests was slightly blunted and (2) the mounting was different. The test model as used by Wentz (1968) was mounted in the tunnel using a single pivot support just forward of the trailing edge and a pitch rod near the apex of the model. The supports were underneath the model wing and retarded the center portion of the flow from underneath the wing. This appears to have had some stabilizing effect on the small vortex system. The slightly blunted apex and the presence of the sting mount appears to have provided less of a stabilizing influence.

Figures 10, 11 and 12 present the percentage change in lift, drag and pitching moment with height above the ground board for the 70 degree delta wing at an angle of attack of 22.1 degrees. As the minimum ground height was approached, the static tests yielded almost 100% increase in lift, 55% increase in drag and 100% increase in pitching moment (negative) over the dynamic test values.

Lift data for the F-104A are given in Figures 13 and 14. In Figure 13 the static wind tunnel data, dynamic wind tunnel data and flight test data show the same trend with change in angle of attack at a given height. The data are nearly of the same magnitude. The increase in lift in ground effect over lift out of ground effect decreases rapidly with increasing angle of attack. A comparison of the F-104A data at a constant angle of attack and changing ground height shows close agreement between the three sets of test data and Lan's (1985) Quasi-Vortex-Lattice Method.

Lift data for the XB-70 are presented in Figures 15, 16 and 17. The dynamic wind tunnel data, Figure 15, shows close agreement with the flight test data at an angle of attack of 9.3 degrees. Below a height of one half wing span above the ground the static wind tunnel data shows a rapid increase in lift over the dynamic data. At an H/b of .2 and .4 and flight test data and the dynamic wind tunnel data show much better agreement than either do with the static wind tunnel test data.

Figure 18 summarizes the ground effect data for the five wings tested at an angle of attack of 12.1 degrees and on H/b of .3 and .4. It can readily be seen that the dynamic effects play an increasing role on lift as sweepback is increased and aspect ratio is decreased. The F-104A data displays only a small variation due to the dynamic conditions. The XB-70 wing, 70 degree delta and the 75 degree delta wings show a large difference between the static and dynamic data.

A tufted wire grid, Figures 7 and 17, behind the 70 degree delta wing was observed during static and dynamic tests by use of a video camera. The locations of the vortex core centers during the tests were determined and plotted as shown in Figures 20 and 21. The dynamic tests were made at a fixed wing angle of attack of 20 degrees. Two sink rates were used to provide induced delta angles of attack of 2 and 4 degrees. The resulting angles of attack of 22 and 24 degrees were then compared with the corresponding static tests. Both comparisons show that the vortices have moved inboard during the dynamic testing relative to the static test positions. The change in vertical position could not be accurately determined.

DISCUSSION

As shown by the results, vortex behavior affects the lift, drag and pitching moment of the wing. The limited tufted wire grid tests demonstrated that vortex lag occurred during the dynamic tests. During these limited visual tests, vortex breakdown did not occur in the proximity of the wing.

Vortex behavior in free air is influenced by a number of items. Wentz (1968) demonstrated the effect of roughness on breakdown and in Schlieren photographs, Figure 22, showed the characteristics of the vortices at breakdown. A free air vortex was sustained by a strong axial core pressure differential by Muirhead (1971, 1977). Also demonstrated were the unsteady nature of the free vortex and its susceptibility to small external pressure differentials perpendicular to the vortex axis. Erickson (1982), Figure 23, illustrated the effect of flaps on vortex behavior. The current reported tests demonstrated that (1) there is a lag in the movement of the wing vortices as the wing moves in ground effect, (2) the forces on the wing during the landing are not those of a wing operating at that angle of attack in steady flight at that height and (3) a change in wind tunnel mounting methods influence vortex behavior. Thus, any change in nearby geometry will cause a change in the behavior of wing vortices. Highly swept low aspect ratio wings appear to be most susceptible to these factors.

A computational simulation model for landing conditions must account for the following (assuming that vortex breakdown may also occur in the vicinity of the trailing edge under unsteady high angle of attack conditions):

- 1) axial core pressure gradient and pressure,
- 2) circulation,
- 3) axial external pressure gradient and pressure,
- 4) pressure gradients transverse to the axis of the vortex.

Further experimental investigations are needed to determine the strength and position of the vortices under various conditions.

A comparison of the limited flight test data on the XB-70, static wind tunnel data and dynamic wind tunnel data indicates that the method of dynamic testing developed provides more realistic data in the landing phase than the static wind tunnel data in ground effect. However, the effect of flaps, fuselage and canard were not accounted for in these tests.

CONCLUSIONS

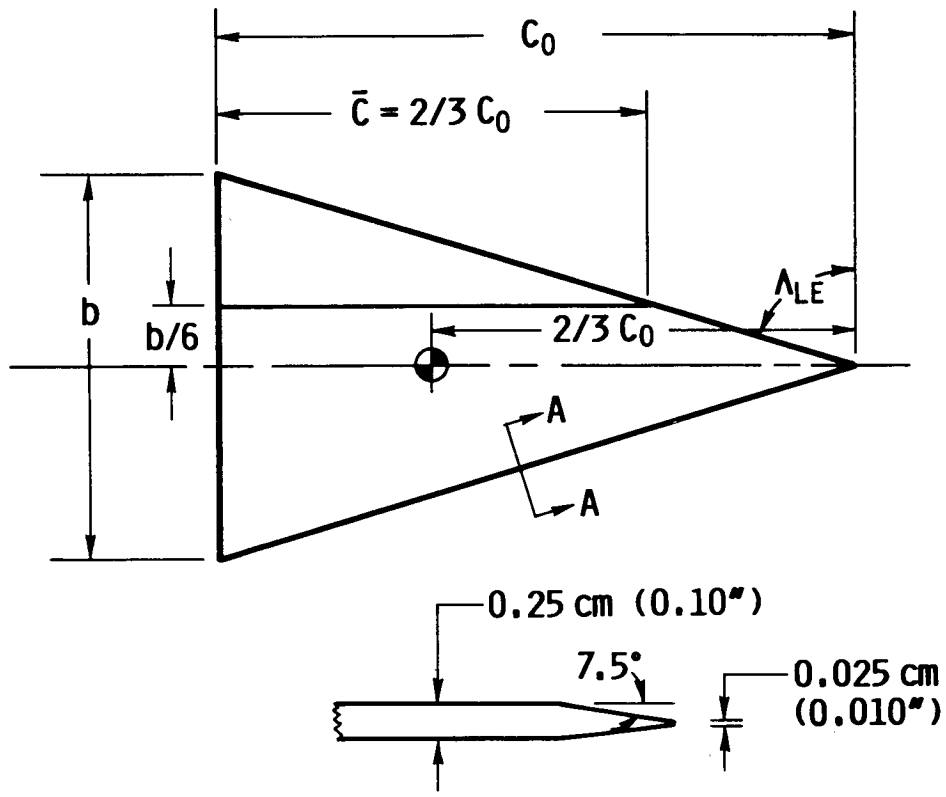
The dynamic wind tunnel simulation which was developed provided a method to simulate the landing condition more realistically than by either static wind tunnel testing in ground effect or constant altitude fly-by testing. The wind-tunnel wing mounting had a distinct effect on the development of vortex breakdown at high angles of attack for the highly swept delta wings.

A significant dynamic effect was found for highly swept delta wings. The wing vortices exhibited a lag during the dynamic tests.

REFERENCES

1. Abercrombie, J. M.; "The Lift of High Circulation Wings in Ground Effect", Saint Louis, Missouri University, Thesis, 1967.
2. Baker, P.; Schweikhard, W.; Young, W.; "Flight Evaluation of Ground Effect on Several Low-Aspect-Ratio Airplanes", NASA TN-D-6053, October 1970.
3. Chang, Ray Chung, "An Experimental Investigation of Dynamic Ground Effect", University of Kansas, Dissertation 1985.
4. Choliassenos, C. J.; "An Experimental Investigation and Theoretical Analysis of the Ground Effect on the Lift of a Wing With and Without Boundary Layer Control", University of Kansas Thesis, 1962.
5. Erickson, Gary E.; "Vortex Flow Correlation", ICAS Paper No. 82-6.6.1; 22-27 August, 1982, Seattle, Washington.
6. Fox, C. H.; "An Analytical Method for Predicting the Lift and Drag for Slender Sharp-Edge Delta Wings in Ground Proximity", M. S. Thesis, Virginia Polytechnic Institute, 1969.
7. Fox, C. H.; "Prediction of Lift and Drag for Slender Sharp-Edge Delta Wings in Ground Proximity", NASA TN-D-4891, 1969.
8. Katz, J; Levin, D.; "Measurements of Ground Effect for Delta Wings", Journal of Aircraft, Vol. 21, No. 6, June 1984.
9. Kemp, W. B.; Lockwood, V. E.; Phillips, W. P.; "Ground Effects Related to Landing of Airplanes With Low-Aspect-Ratio Wings", NASA TN D-3583, October 1966.
10. Lan, C. E.; "VORSTAB - A Computer Program for Calculating Lateral-Directional Stability Derivatives With Vortex Flow Effect", NASA CR-172501, January 1985.
11. Muirhead, V. U.; Eagleman, J. R.; "Laboratory Compressible Flow Tornado Model", Preprints Seventh Conference on Severe Local Storms, AMS, Kansas City, Missouri 1971.

12. Muirhead, V. U.; "Investigation of Compressible Vortex Flow Characteristics", NASA CR-145261, 1977.
13. Rolls, L. S.; Koenig, D. G.; "Flight Measured Ground Effect on a Low-Aspect-Ratio Ogee Wing Including a Comparison With Wind-Tunnel Results", NASA TN D-3431, 1966.
14. Schweikhard, W.; "A Method for In-Flight Measurement of Ground Effect on Fixed-Wing Aircraft", Journal of Aircraft, Vol. 4, No. 2, March-April, pp. 101-104.
15. Tani, I.; Taima, M.; Simidu, S.; "The Effects of Ground on the Aerodynamic Characteristics of a Monoplane Wing", Tokyo Imperial University, Aero Research Inst. Rept. 156, September 1937.
16. Weiselsberger, C.; "Wing Resistance Near the Ground", NACA TM77, April 1922.
17. Wentz, W. H.; "Wind-Tunnel Investigations of Vortex Breakdown on Slender Sharp-Edge Wing", Ph. D. Dissertation, University of Kansas, 1968.



Wing Model	60° Delta	70° Delta	75° Delta
Root Chord, C_0 cm (in)	22.00 (8.66)	34.90 (13.74)	45.72 (18.00)
Span, b cm (in)	25.40 (10.00)	25.40 (10.00)	24.49 (9.64)

Figure 1. Model Geometry, Delta Wings

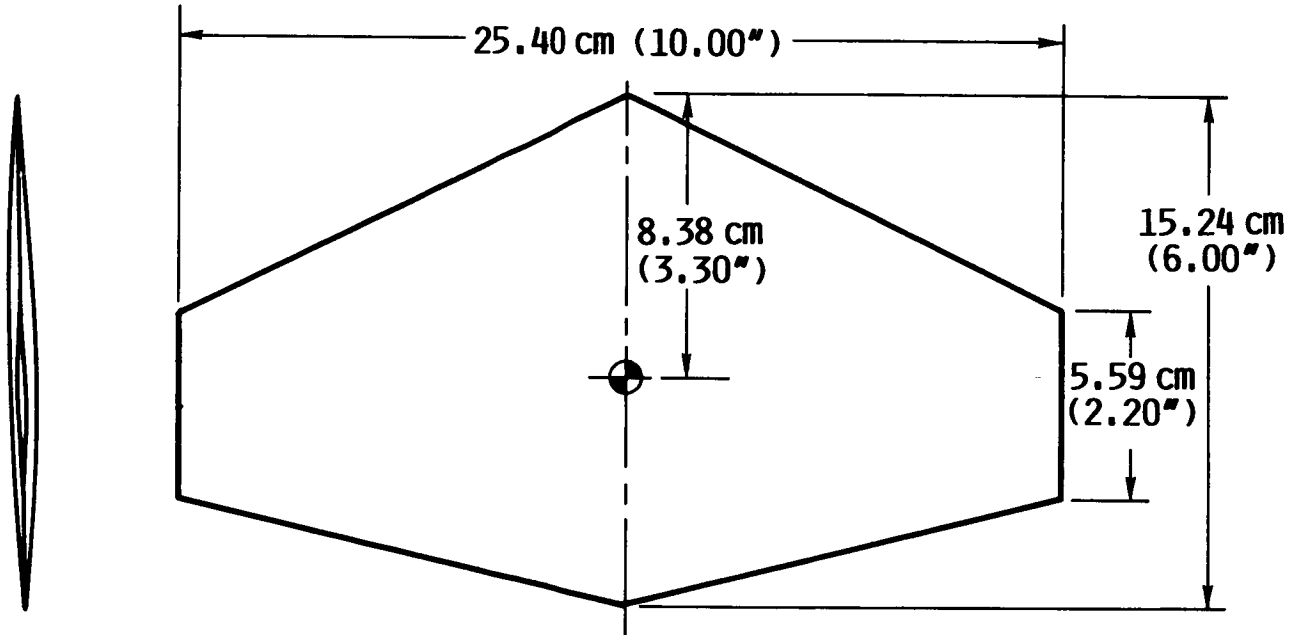


Figure 2. Model Geometry, F-104A Wing

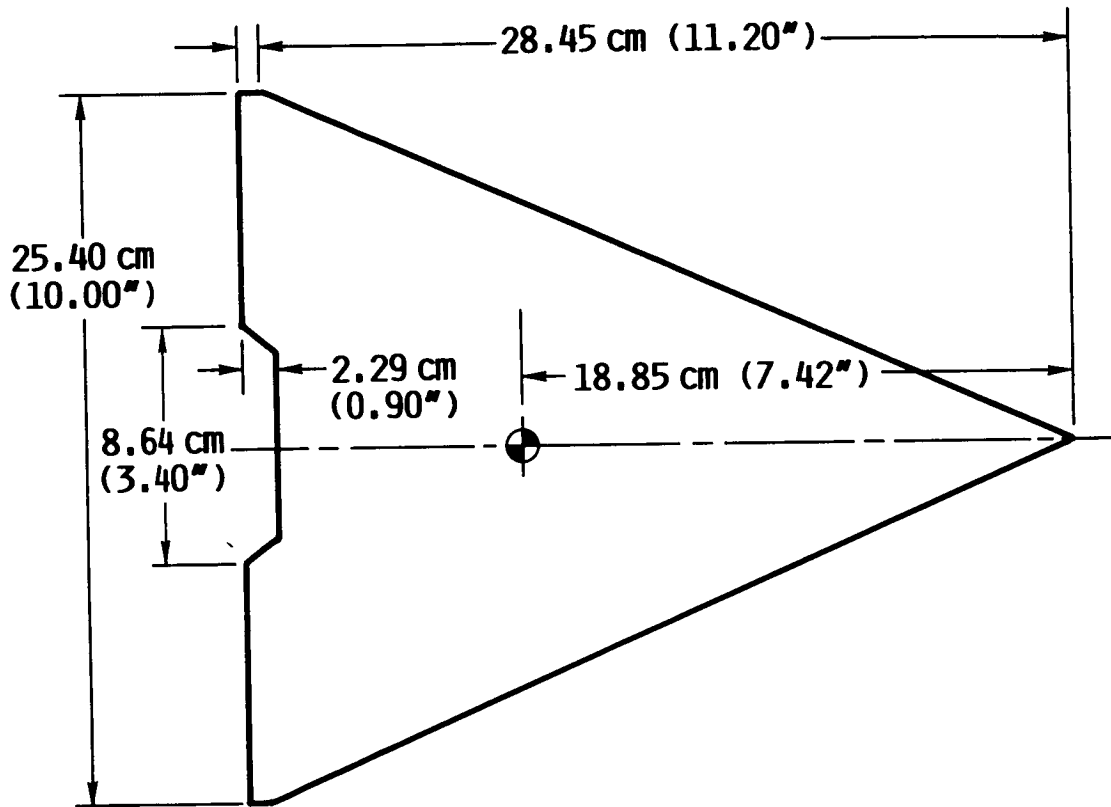


Figure 3. Model Geometry, XB-70 Wing

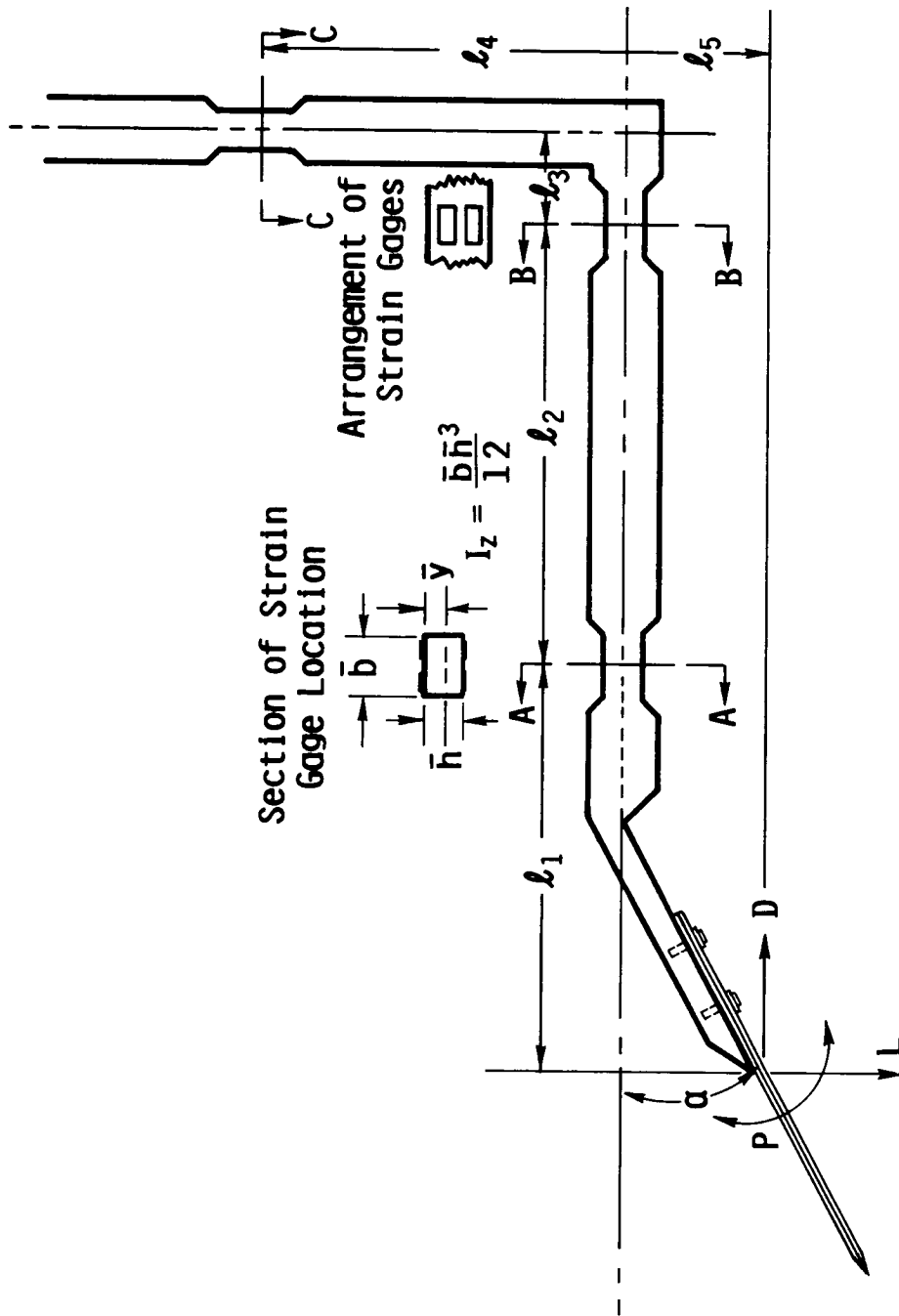


Figure 4. Sting Support and Strain Gage Arrangement

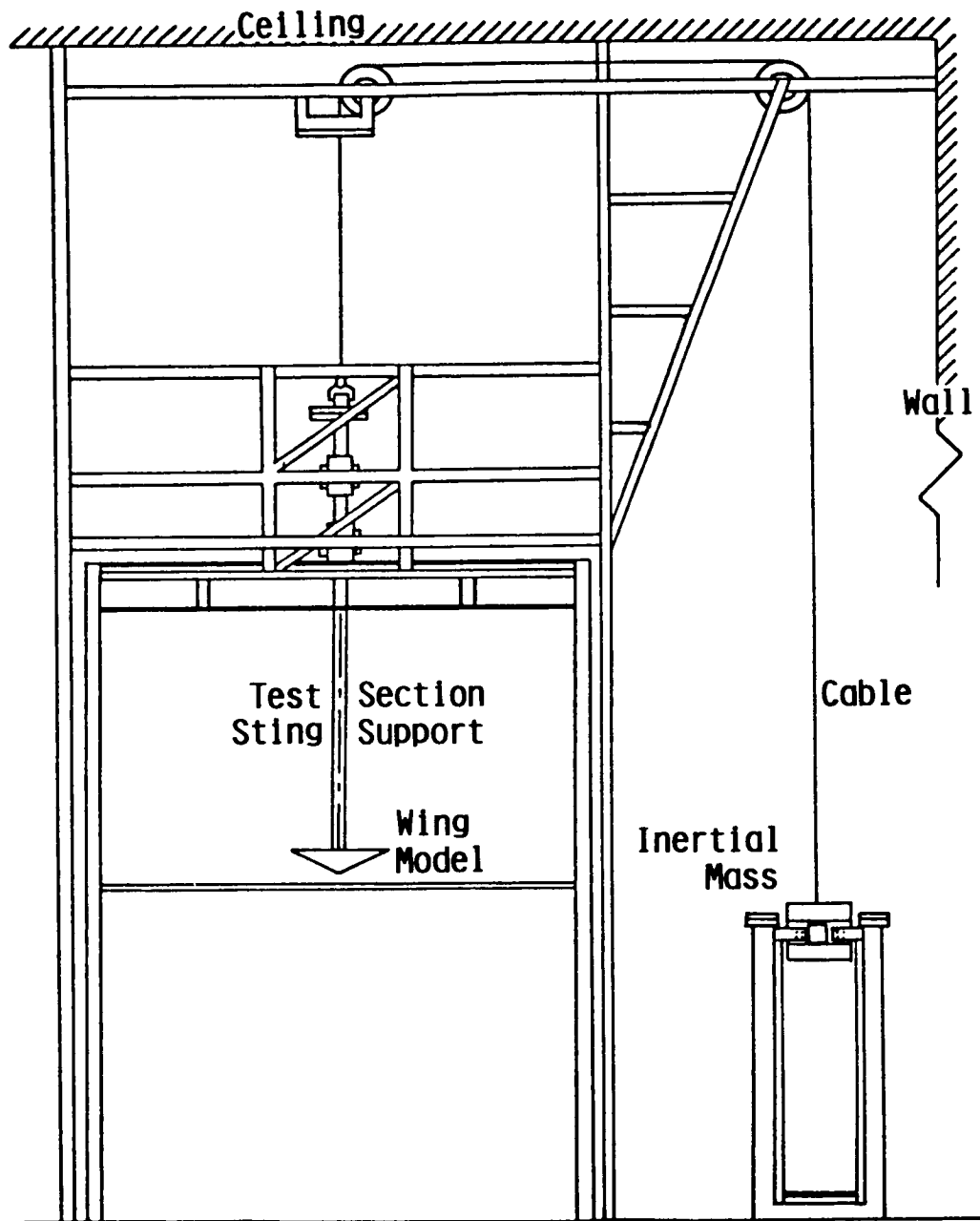


Figure 5. Airstream View of Test Stand

ORIGINAL PAGE IS
OF POOR QUALITY



Figure 6. Flow Visualization Using Helium Bubbles

ORIGINAL PAGE IS
OF POOR QUALITY

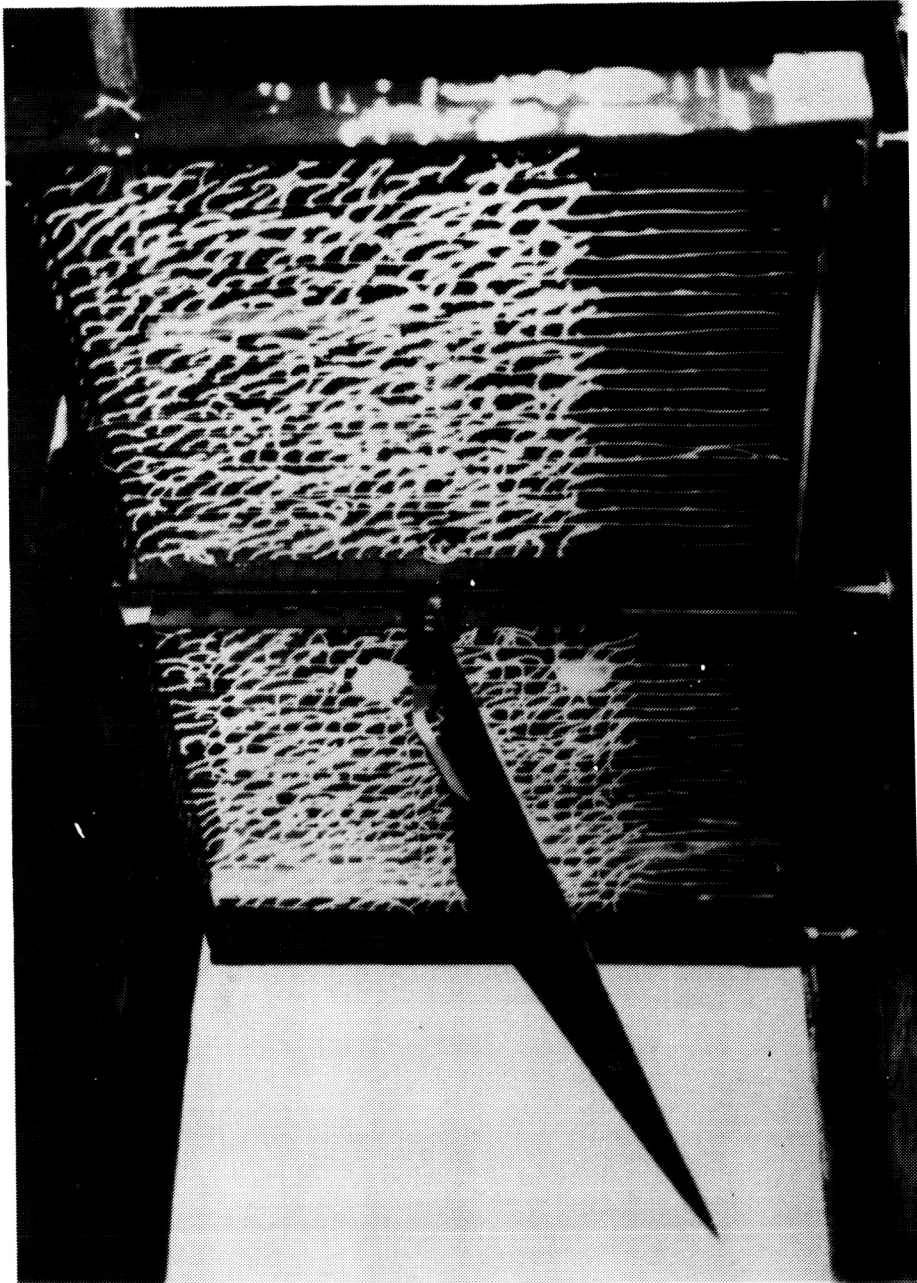


Figure 7. A Photograph of Tufted Wire Grid

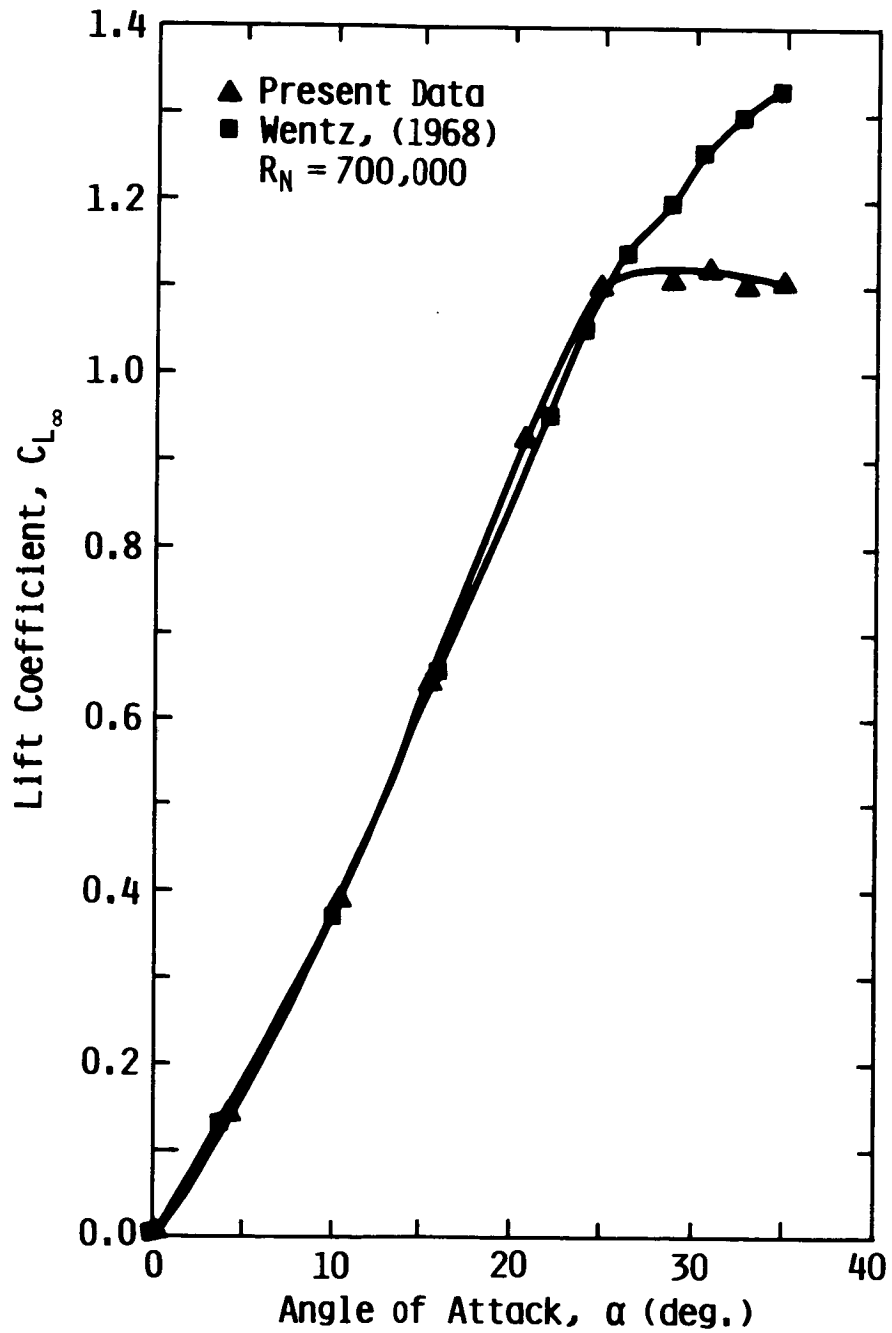


Figure 8. Comparison of Present Out-of-Ground-Effect Lift Coefficient Data for 70 Degree Delta Wing with Wentz's Data (1968)

References as in Reference - Erickson, 1982		R_N Based on C_0	
○	Reference 34	Water Tunnel	4.1×10^4
●	Reference 147	Water Tunnel	9.8×10^3
+	Reference 139	Water Tunnel	1.0×10^4
□	Reference 148	Wind Tunnel	1.5×10^6
△	Reference 148	Wind Tunnel	1.3×10^6
→ ●	Reference 109	Wind Tunnel	9.0×10^5
×	Reference 149	Wind Tunnel	$1.4 \& 1.7 \times 10^6$
△	Reference 77	Wind Tunnel	2.0×10^6
◇	Reference 148	Flight	40.0×10^6
◆	Reference 26	Water Tunnel	$1.0 \& 8.0 \times 10^4$
*	Reference 151	Wind Tunnel	2.0×10^6
▲	Reference 150	Wind Tunnel	1.0×10^6
◆	Reference 148	Water Tunnel	3.0×10^4
⊠	Reference 27	Water Tunnel	3.0×10^4
—	Current Data	Wind Tunnel	7.0×10^5

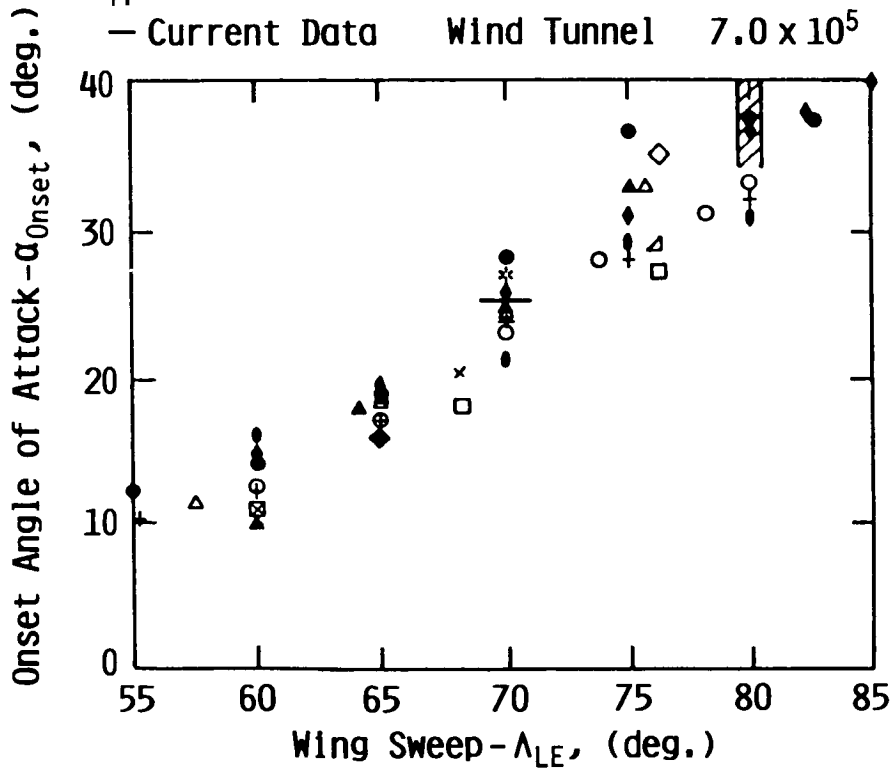


Figure 9. Effects of Wing Sweep and Reynolds Number on Delta Wing Vortex Breakdown at the Trailing Edge (Erickson, 1982) & (Wentz, 1968) (→ Wentz, 1968)

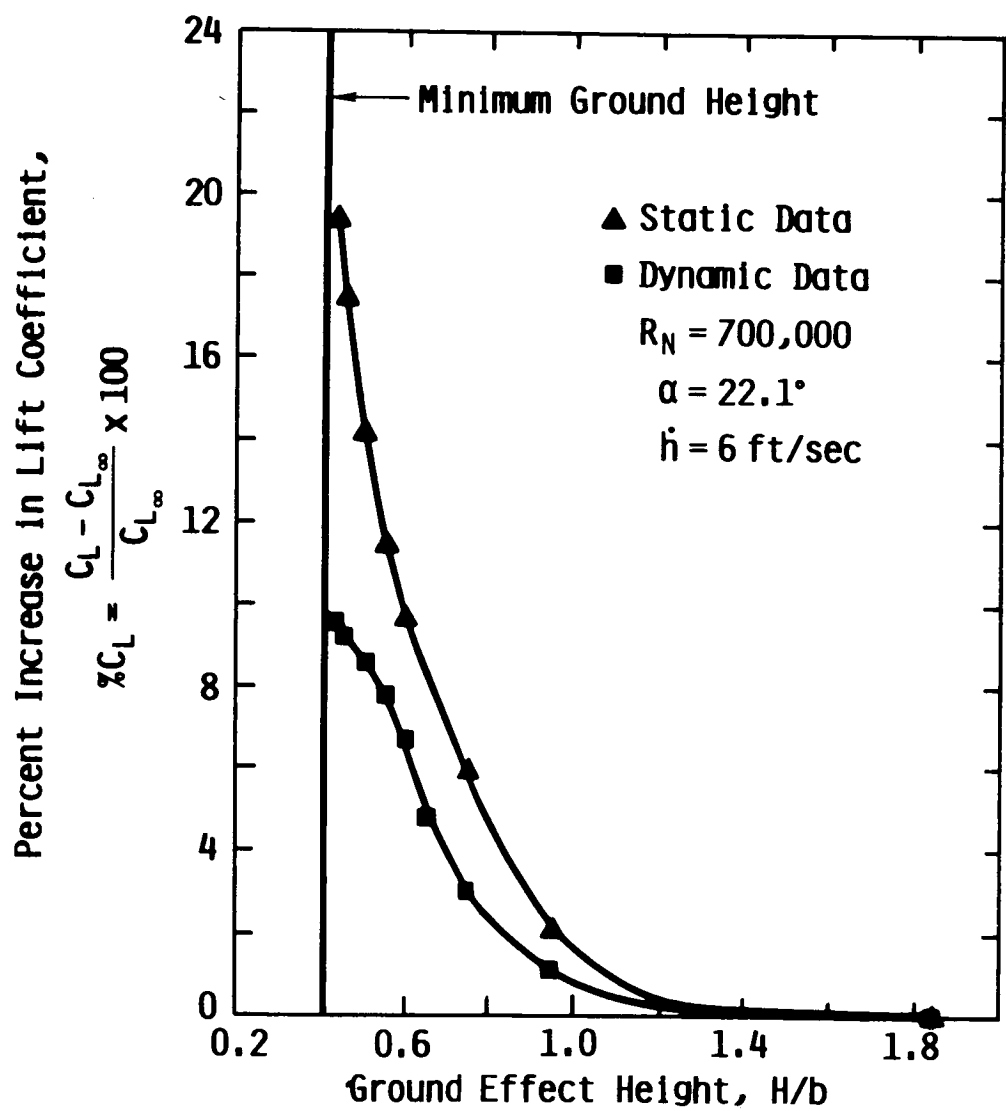


Figure 10. Comparison of Lift Increments for Static and Dynamic KU Wind Tunnel Ground Effect Data for 70 Degree Delta Wing at 22.1 Degree Angle of Attack

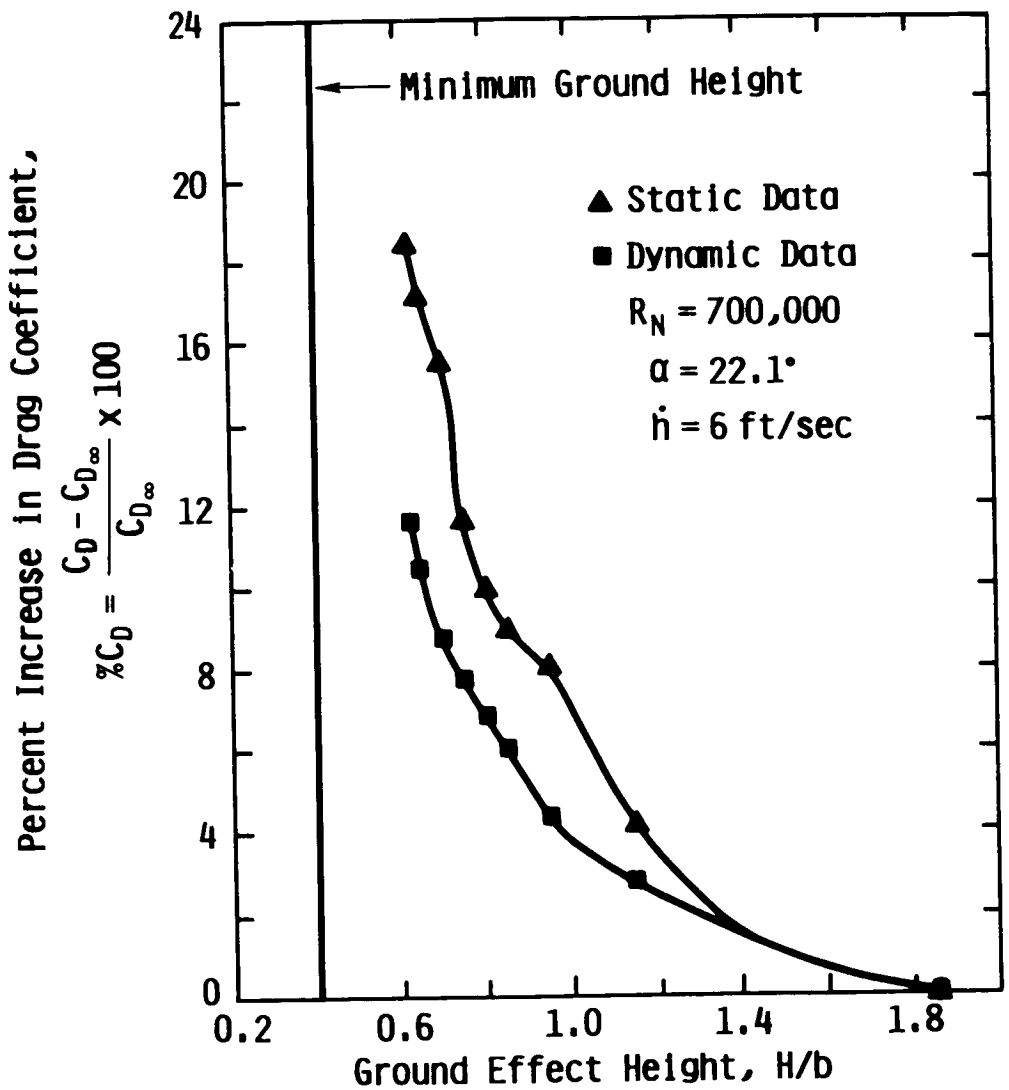


Figure 11. Comparison of Drag Increments for Static and Dynamic KU Wind Tunnel Ground Effect Data for 70 Degree Delta Wing at 22.1 Degree Angle of Attack

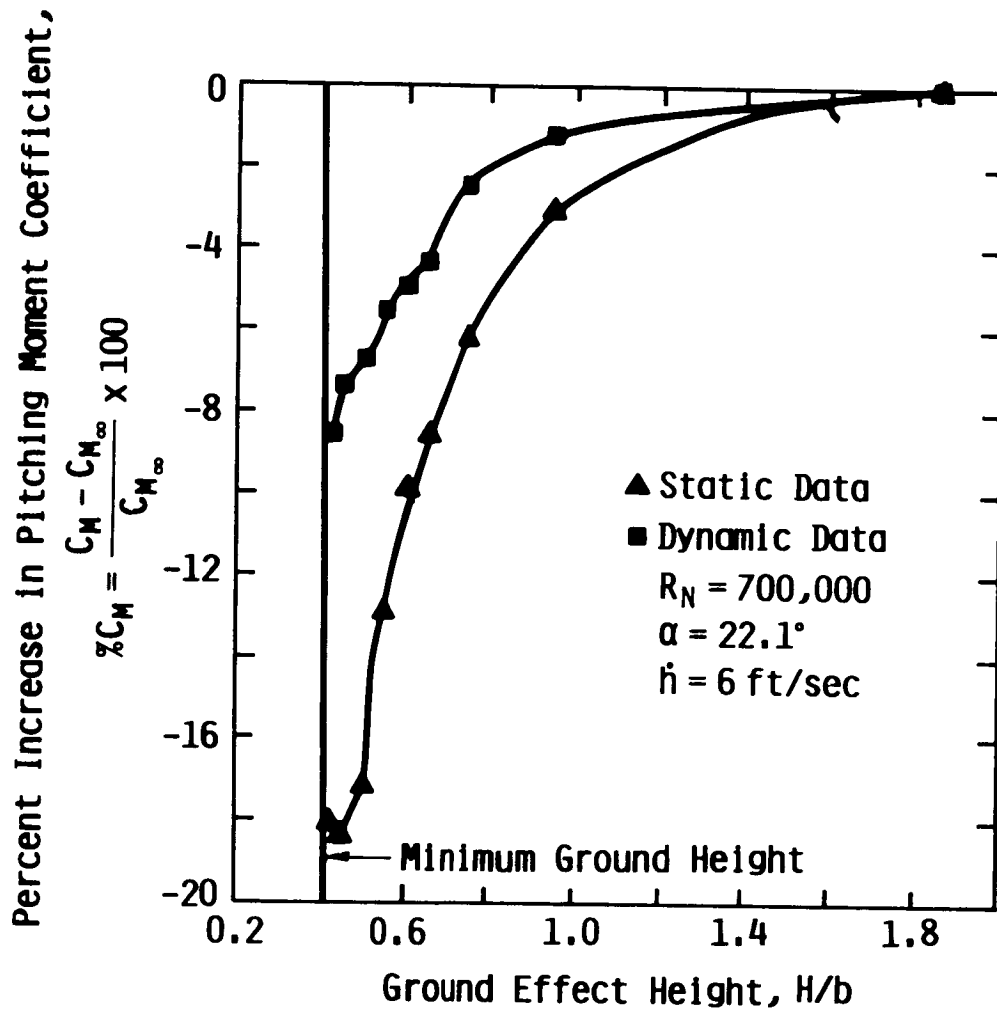


Figure 12. Comparison of Pitching Moment Increments for Static and Dynamic KU Wind Tunnel Ground Effect Data for 70 Degree Delta Wing at 22.1 Degree Angle of Attack

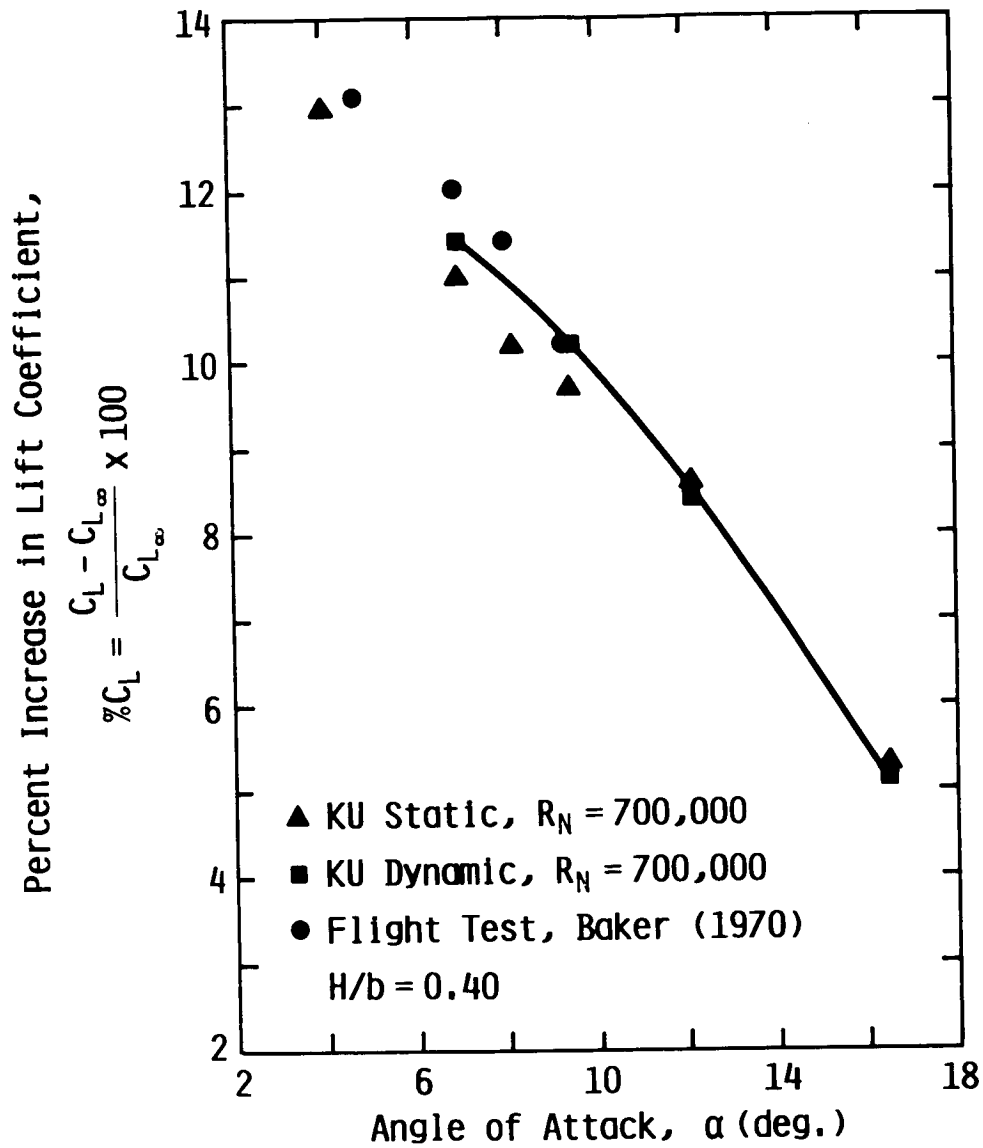


Figure 13. Comparison of Lift Increments for Static and Dynamic Wind Tunnel (Wing Model) Data with Flight Test Data for F-104A, $H/b = 0.40$

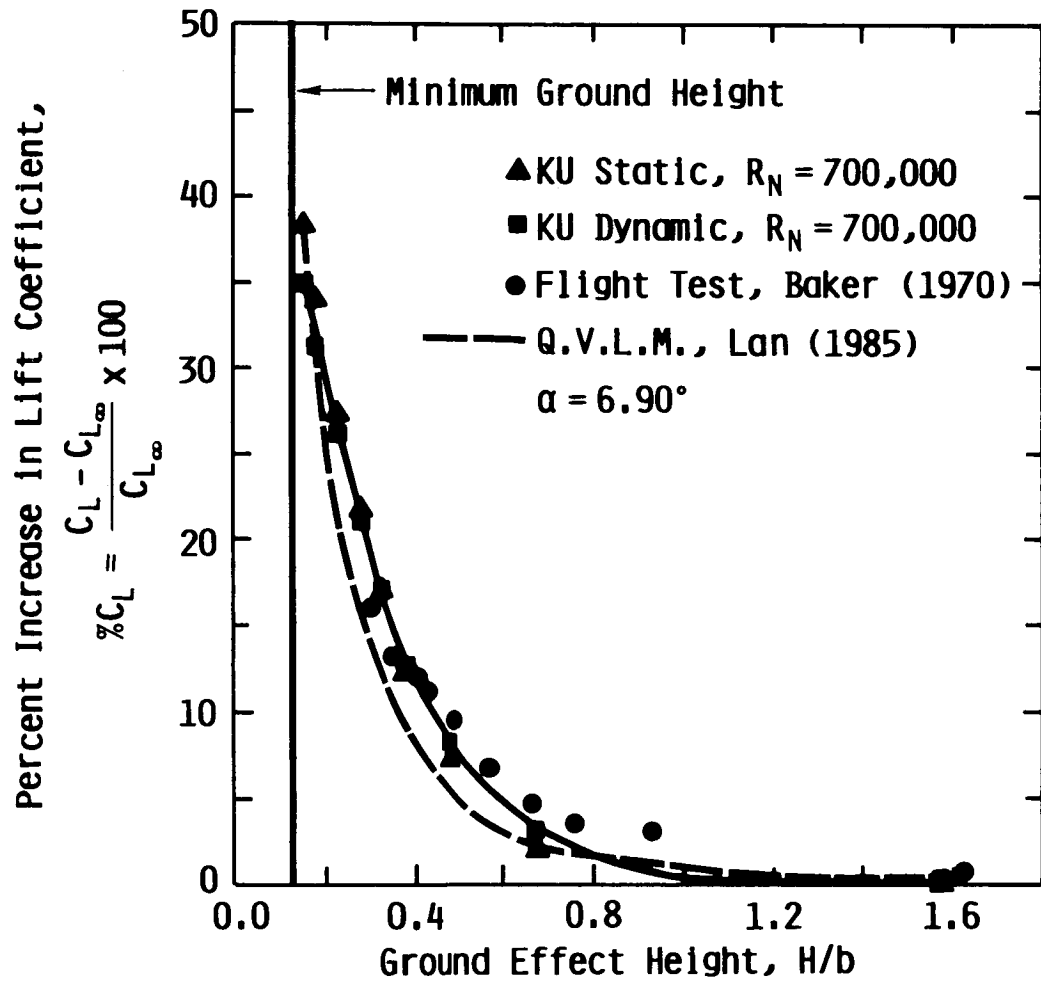


Figure 14. Comparison of Lift Increments for Static and Dynamic Wind Tunnel Data (Wing Model) with Flight Test (Airplane) and Q.V.L.M. (Wing Model) Data for F-104A, at 6.9 Degree Angle of Attack

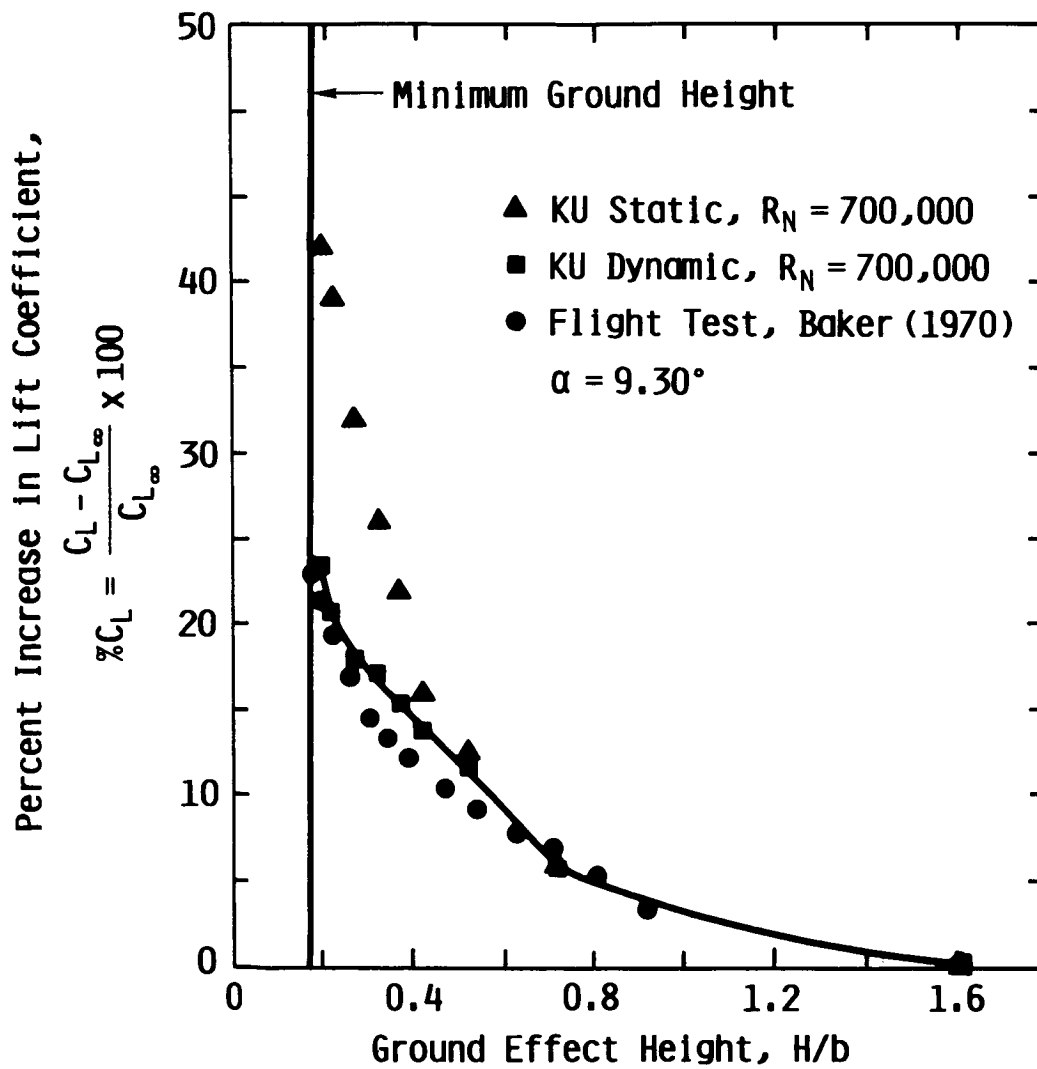


Figure 15. Comparison of Lift Increments for Static and Dynamic Wind Tunnel (Wing Model) Data with Flight Test Data for XB-70 at 9.3 Degree Angle of Attack

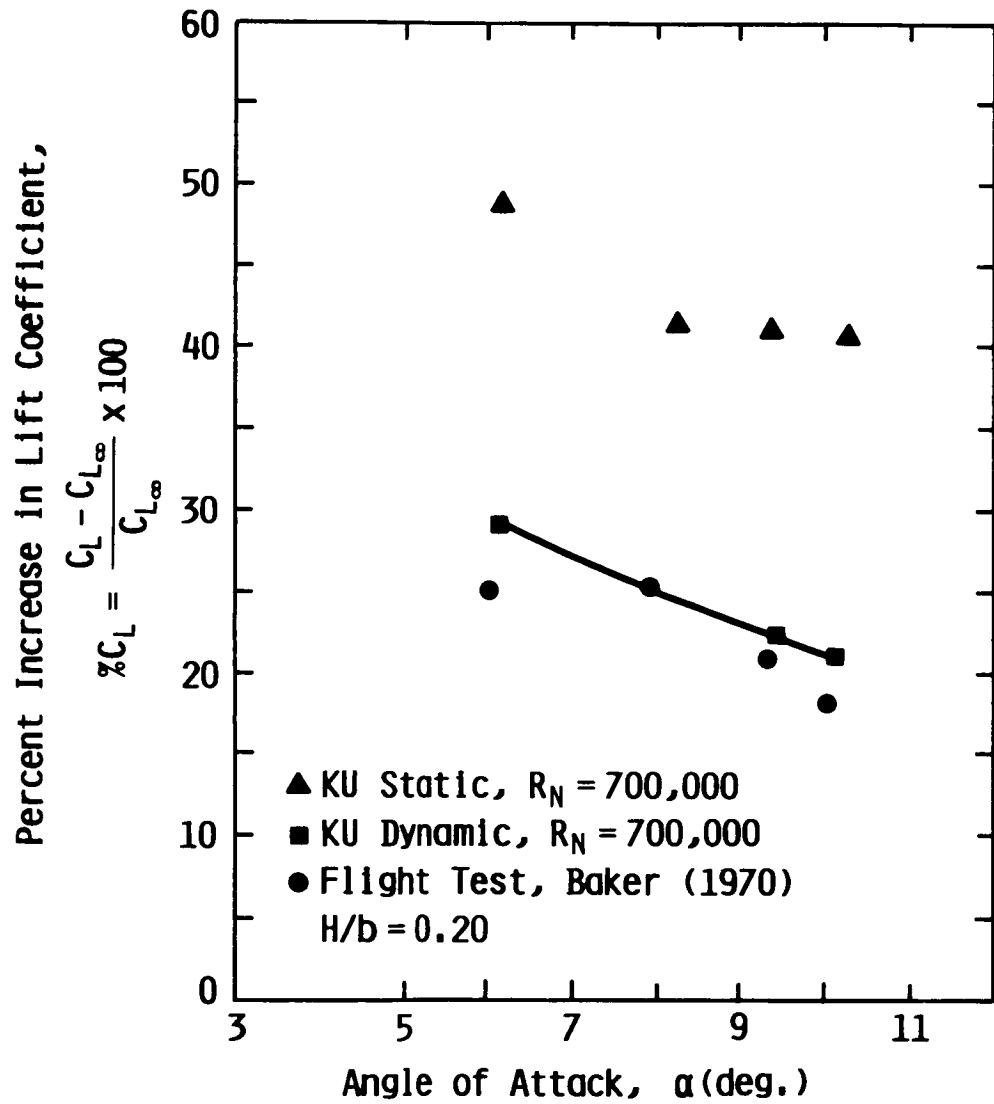


Figure 16. Comparison of Lift Increments for Static and Dynamic Wind Tunnel (Wing Model) Data with Flight Test Data for XB-70, $H/b = 0.20$

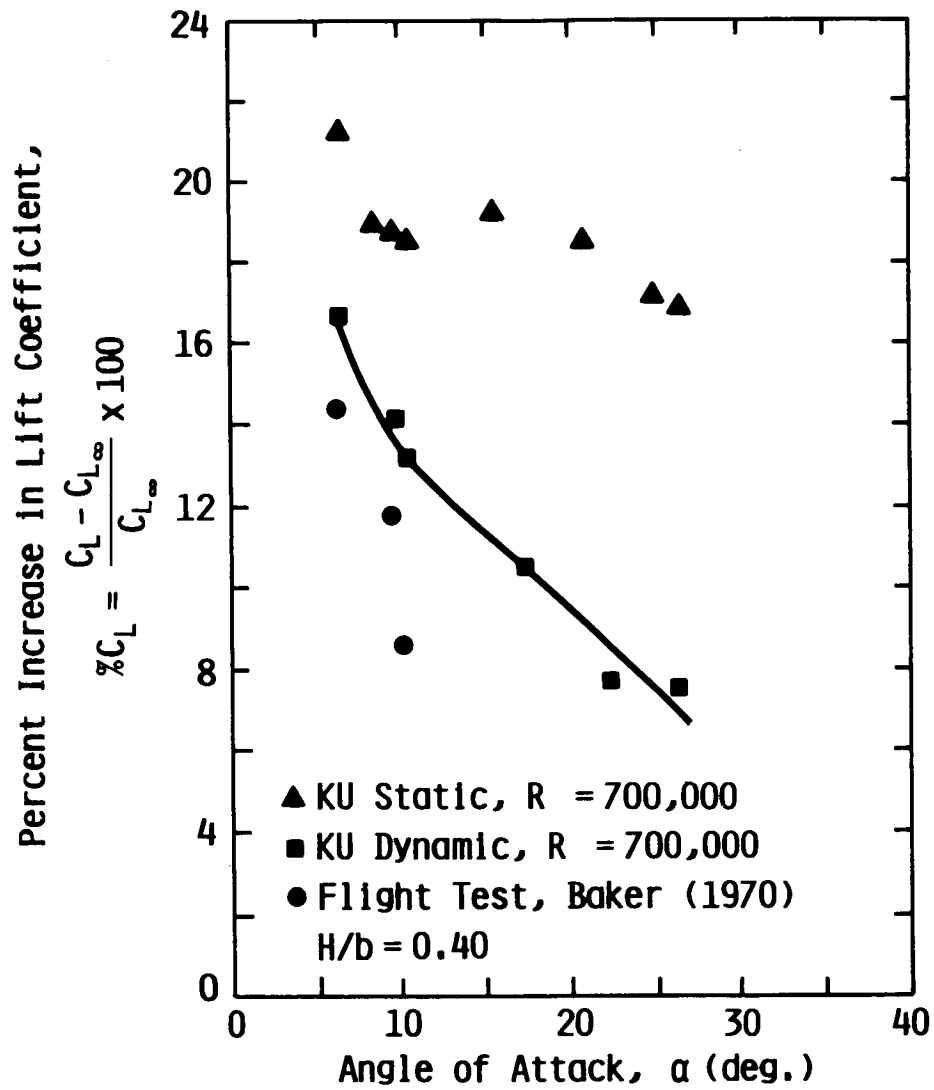


Figure 17. Comparison of Lift Increments for Static and Dynamic Wind Tunnel (Wing Model) Data with Flight Test Data for XB-70, $H/b = 0.40$

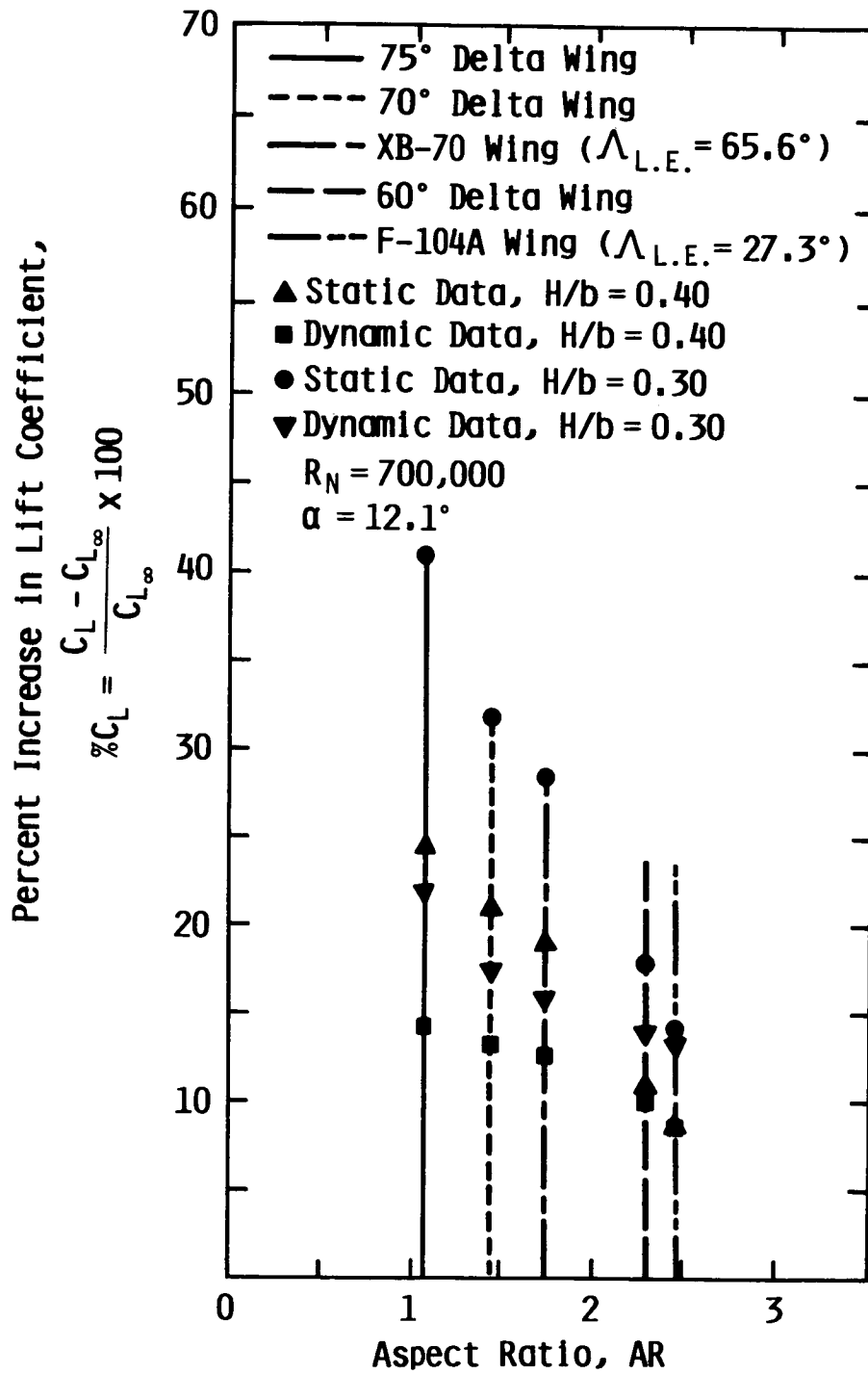


Figure 18. Variation of Incremental Lift Coefficient with Aspect Ratio for Static and Dynamic KU Ground Effect Data at 12.1 Degree Angle of Attack

ORIGINAL PHOTO IS
OF POOR QUALITY

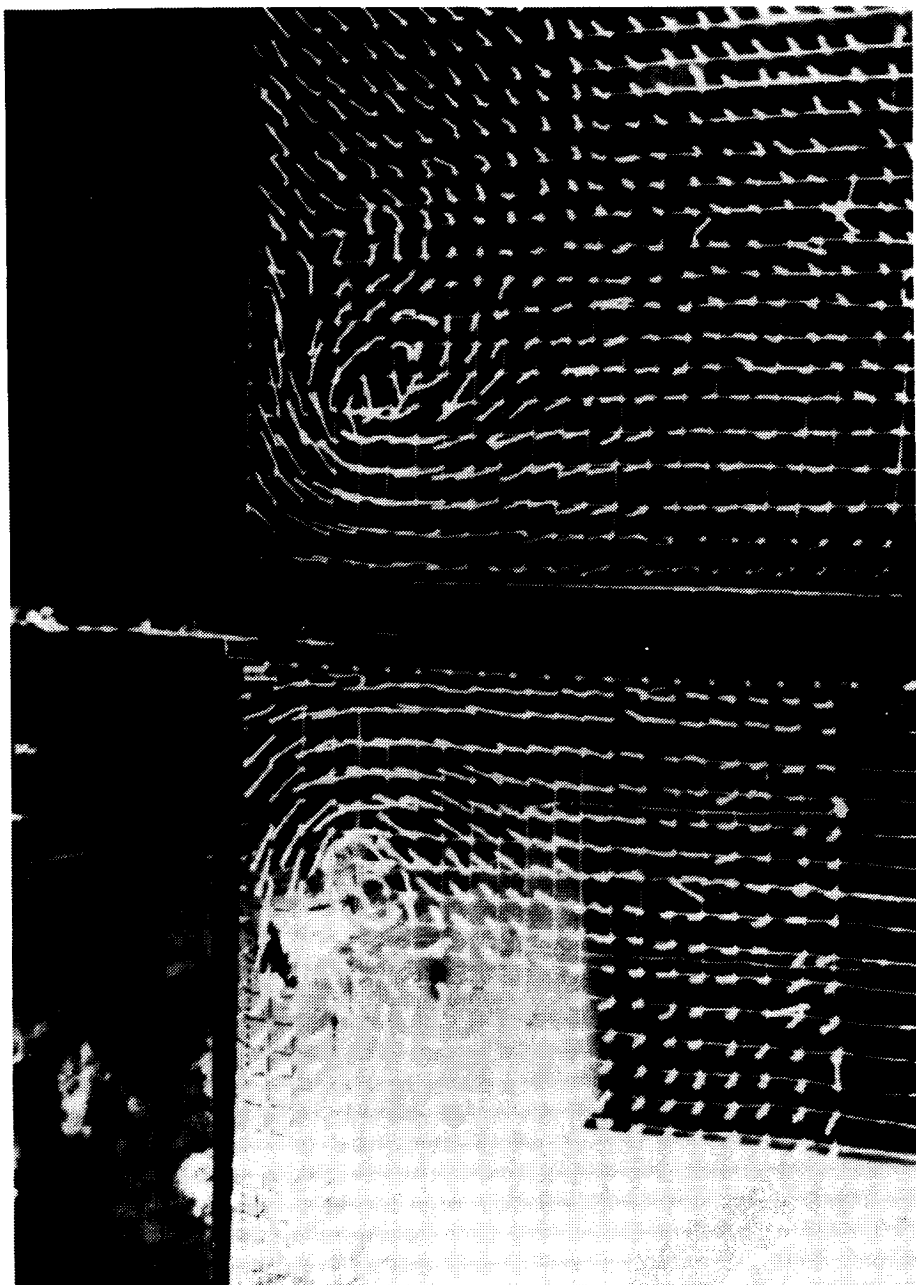


Figure 19. A Photograph of Tufted Vortex Visualization

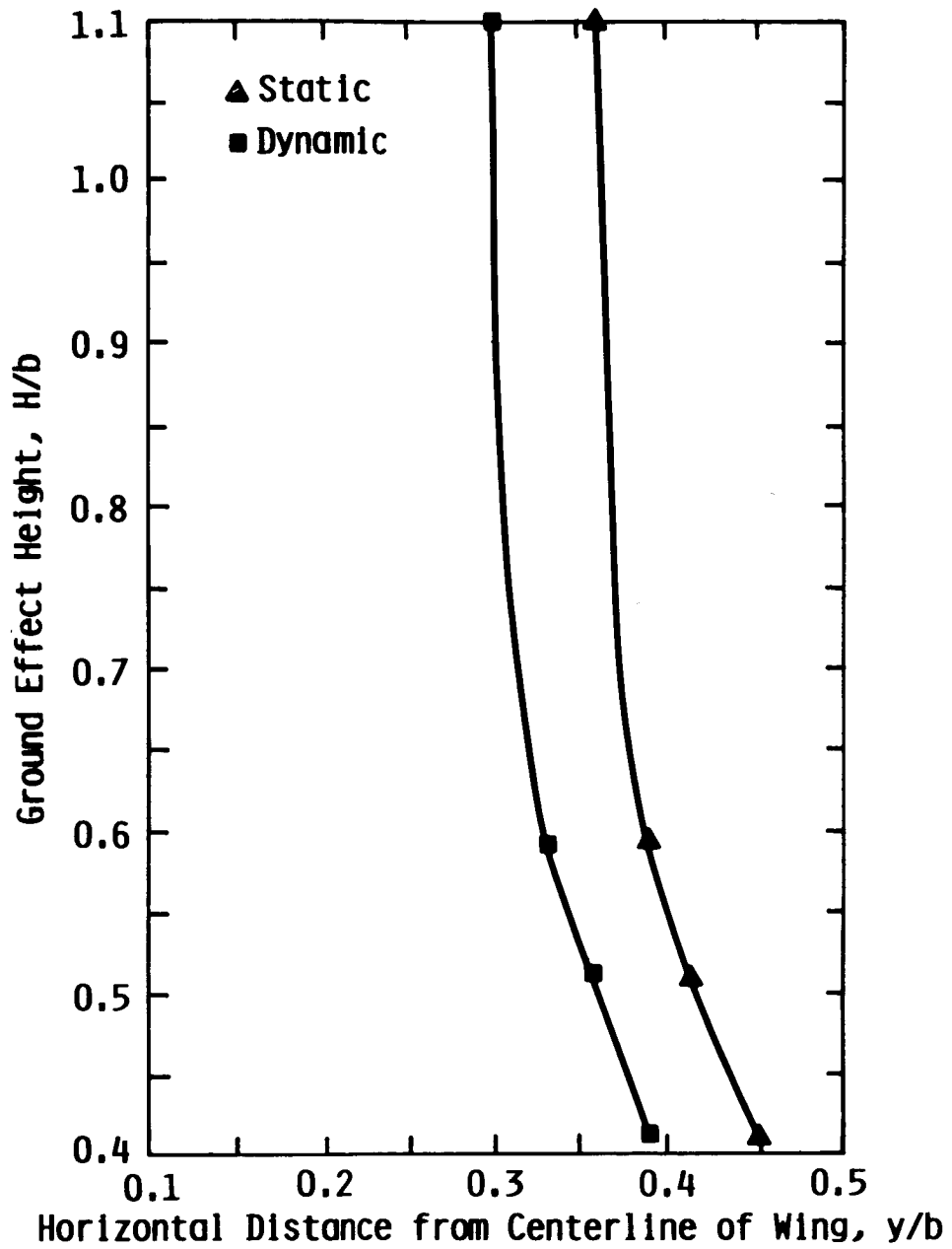


Figure 20. Comparison of Location of the Vortex Core Center for Static and Dynamic Ground Effect, for 70 Degree Delta Wing at 22 Degree Angle of Attack

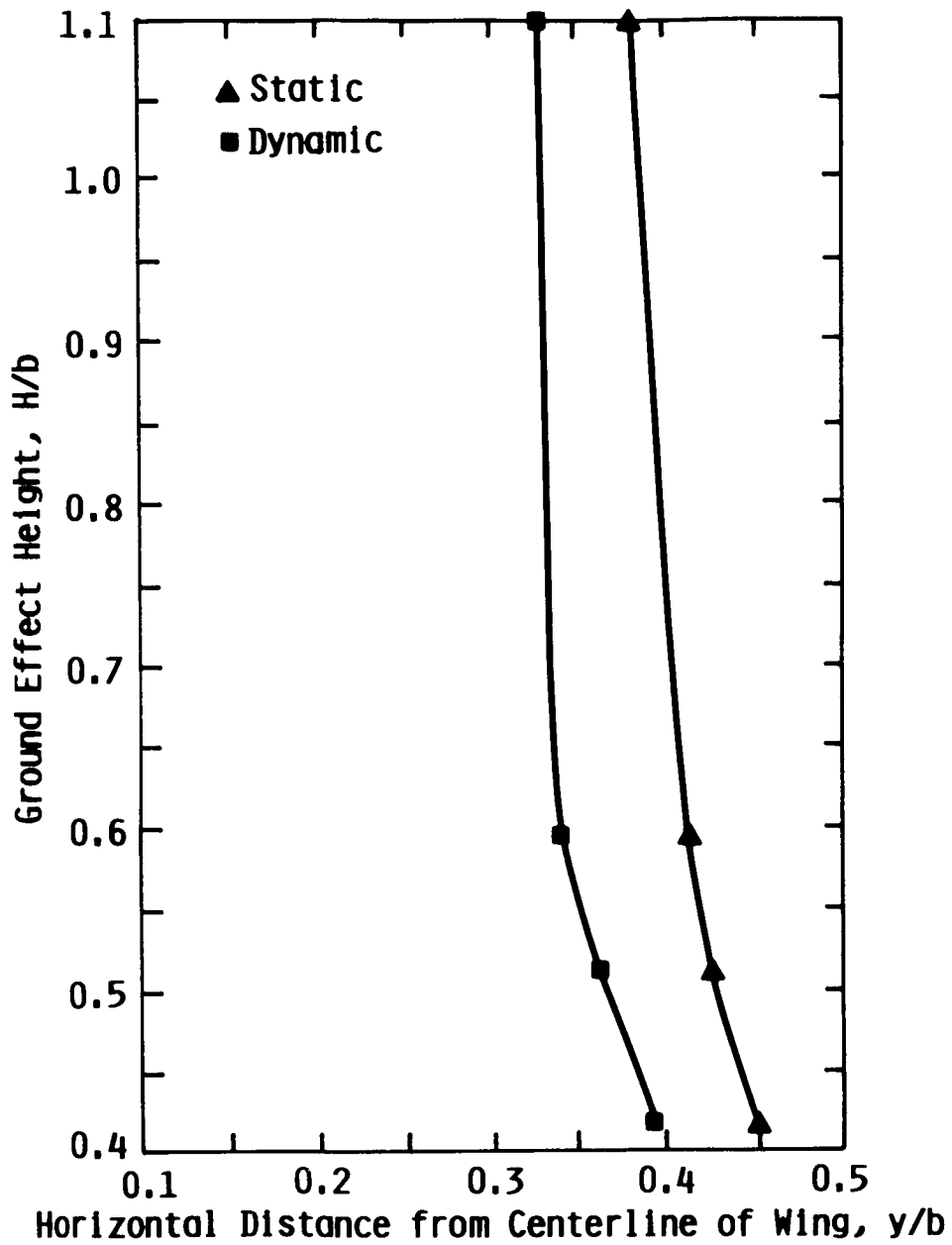
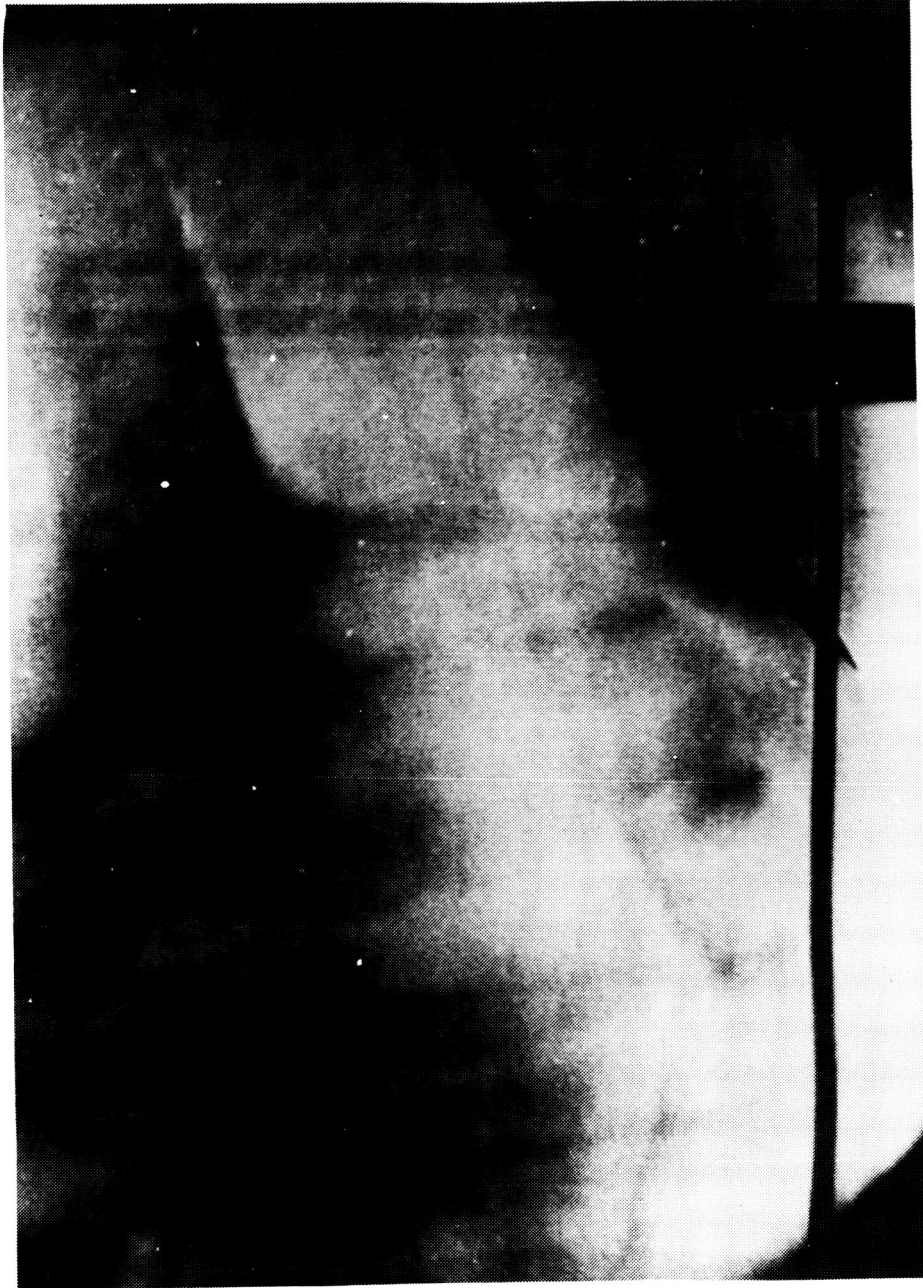


Figure 21. Comparison of Location of the Vortex Core Center for Static and Dynamic Ground Effect, for 70 Degree Delta Wing at 24 Degree Angle of Attack

ORIGINAL PAGE IS
OF POOR QUALITY



$\alpha = 27.5^\circ$ No Breakdown

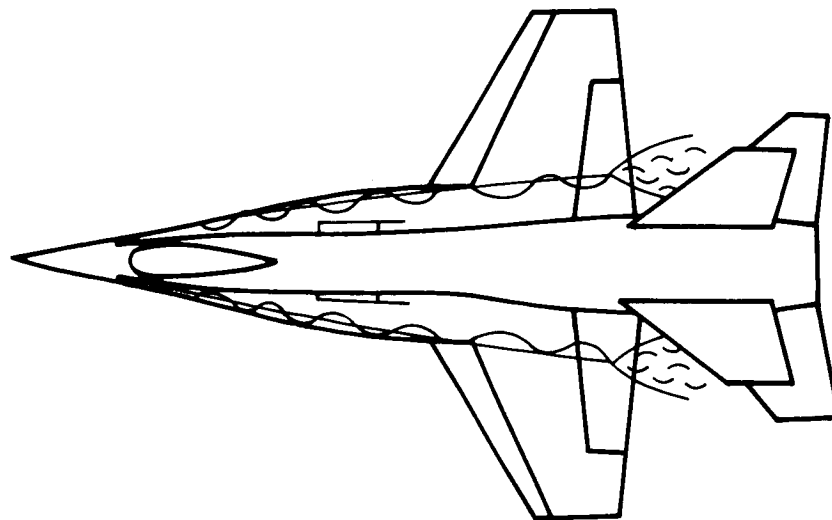
Figure 22a. Effect of Roughness on Breakdown Characteristics (72.5° Delta Wing)
(Wentz, 1968)

ORIGINAL PAGE IS
OF POOR QUALITY

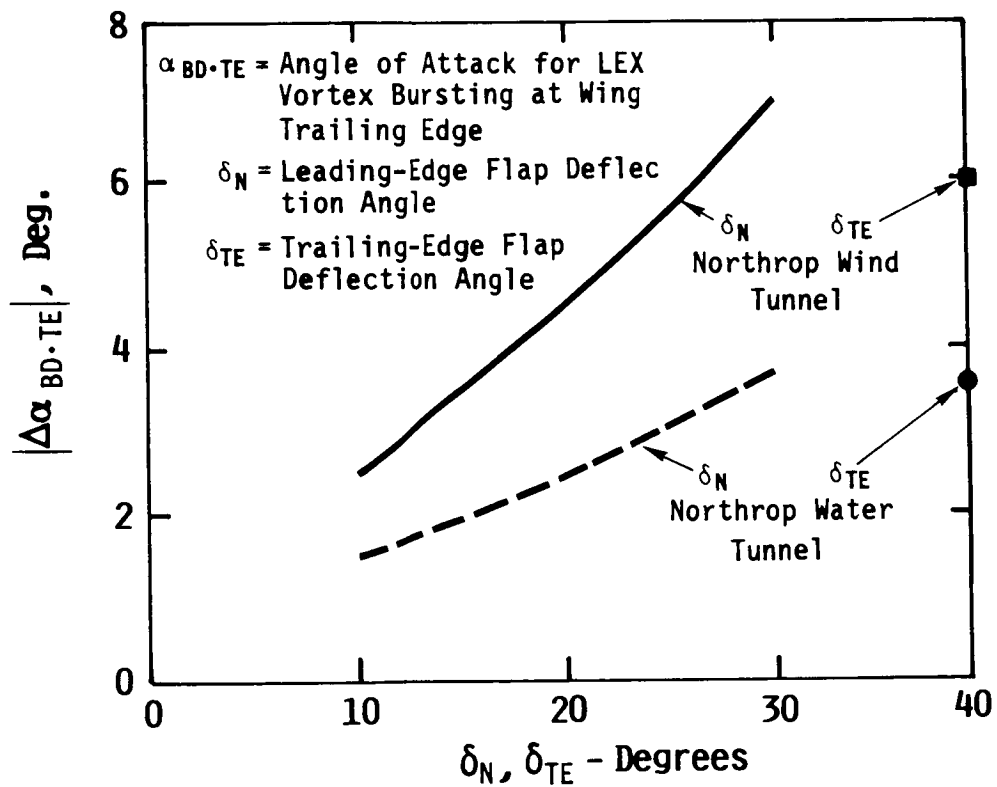


$\alpha = 32.5^\circ$ Breakdown

Figure 22b. Effect of Roughness on Breakdown Characteristics (72.5° Delta Wing)
(Wentz, 1968)



(a) Sketch of Northrop P-530 Wind Tunnel Model



(b) Effects of Leading- and Trailing-Edge Flaps on Lex Vortex Stability

Figure 23. Deflected-Flap Effects on Vortex Behavior (Erickson, 1982)